Available online at www.sciencedirect.com
ScienceDirect
Journal of Computational Physics 218 (2006) 495–509
JOURNAL OF COMPUTATIONAL PHYSICS
www.elsevier.com/locate/jcp

Robustness of MUSCL schemes for 2D unstructured meshes

Christophe Berthon

MAB UMR 5466 CNRS, Université Bordeaux I, 351 cours de la libération, 33400 Talence, France
INRIA Futurs, Labri, Projet ScAlApplix, 351 cours de la libération, 33400 Talence, France

Received 17 May 2005; received in revised form 10 February 2006; accepted 21 February 2006
Available online 19 April 2006

Abstract

We consider second-order accuracy MUSCL schemes to approximate the solutions of hyperbolic system of conservation laws. In the context of the 2D unstructured grids, we propose a limitation procedure on the gradient reconstruction to enforce several stability properties. We establish that the MUSCL scheme preserves the invariant domains and satisfy a set of entropy inequalities. A conservation assumption is not useful in the present work to define the piecewise linear approximations and the proposed limitation can be understood as a systematic correction of the standard gradient reconstruction procedure. The numerical method is applied to the compressible Euler equations. The gradient reconstruction is performed using the characteristic variables. Several numerical tests exhibit stability and robustness of the scheme.

Keywords: Finite volume method; MUSCL scheme; Unstructured meshes; Invariant region; Discrete entropy inequalities; Compressible Euler equations

1. Introduction

This paper deals with the numerical approximations for solving multidimensional hyperbolic system of conservation laws on unstructured grids. Following the ideas of Perthame–Qiu [23], we propose to discuss a variant of the well-known MUSCL scheme introduced by Van Leer [21]. This scheme is a finite volume method where the flux approximation is second-order accuracy and has been leading several researches in this topic (see [8,10,27]). In the MUSCL approaches, a slope limitation is introduced when computing the gradients. A large literature is devoted to this limitation useful to avoid numerical oscillations (for instance, see [25] or [26]) as for scalar conservation laws because of the TVD properties (see [14]). As soon as systems of conservation laws are considered, these limitations turn out to be very unnatural since the TVD properties are thus wrong.

In the work of Perthame–Qiu [23], the authors propose to substitute the usual gradient reconstruction by interpolations to consider a piecewise constant approximation on sub-cell and not a piecewise linear function by cell. Next, they impose a limitation based on a conservation argument and they prove several stability properties satisfied by the scheme. Owing a recent work of Berthon [3], we establish that classical MUSCL

E-mail address: Christophe.Berthon@math.u-bordeaux.fr.

0021-9991/$ - see front matter
doi:10.1016/j.jcp.2006.02.028

scheme (see [21] but also [12] or [29]) based on a gradient reconstruction and the Perthame–Qiu variant based on the interpolated values coincide. This leads us to introduce a MUSCL scheme where the limitation step does not involve a conservation property like in [23]. This states the very discrepancy with the other stable limitations procedure or relevant variants [23] where conservation of the gradient reconstruction is imposed.

Another motivation for this interpretation of the MUSCL scheme is given by physical arguments. Indeed, in the present work, we consider hyperbolic system in the form

$$\partial_t \mathbf{W} + \mathrm{div}\mathbf{F}(\mathbf{W}) = 0, \quad x \in \mathbb{R}^2, \ t > 0, \tag{1}$$

where the state vector $\mathbf{W}$ belongs to a convex set $\mathscr{V}$, assumed to be invariant by the flow. In general, the invariance of $\mathscr{V}$ coincides with physical assumptions (for instance, positive density and pressure). Considering a relevant CFL restriction for the second-order MUSCL scheme, we are able to ensure the numerical invariance of $\mathscr{V}$. Such a stability property is crucial for a large number of numerical simulations: strong shock interaction, low density, multiphase models (for instance see [16] or [18]), non thermodynamical equilibrium flows [4]. From now on, let us emphasise that this stability property just requires to use a numerical scheme which preserves the invariant region for the one-dimensional first-order problems (with a gradient reconstruction value fixed to zero).

This first stability property is next completed by a set of discrete entropy inequalities. Indeed, we assume that the weak solutions of (1) satisfy the following entropy inequality (see [19,20]):

$$\partial_t S(\mathbf{W}) + \mathrm{div}\,\mathscr{F}(\mathbf{W}) \leqslant 0, \tag{2}$$

where $\mathbf{W} \to S(\mathbf{W})$ denotes a convex application. With no additional limitation on the gradient reconstruction, we prove that approximate solutions by a MUSCL scheme satisfy a discrete form of (2). In addition, let us note that results concerning the minimum entropy principle (see [28], but also [17]) satisfied by both Euler equations and several derived models are given (see [4]).

The paper is organized as follows. In the following section, we describe the second-order multidimensional scheme on an unstructured grid. This description will be very short since the considered scheme is very usual (see [12,17,23]). This presentation is concluded by an interpretation of the gradient reconstruction which follows the idea introduced by Perthame–Qiu [23] (see also [2]). In Section 3, we give the expected stability result concerning the invariance of the domain $\mathscr{V}$ and the entropy inequalities. These results are stated in the general context and the assumptions made on the gradient reconstruction will be weaker as possible. The following section is devoted to numerical applications where the Euler equations are considered. The MUSCL scheme will be based on the Suliciu relaxation scheme (see [5,6] or [2,4] to further details, see also [15] to a description of the initial relaxation scheme) and the gradient reconstruction will be performed using the characteristic variables. Several numerical simulation, involving low density and strong shock waves, illustrate the method. A brief conclusion achieved the paper.

2. Description of the scheme

In this section, we propose a brief description of the MUSCL scheme for an unstructured mesh. At this level of the paper, we do not introduce innovative results and we use the usual approaches (see [12] or [23] and references therein to further details).

First, we describe the grid uses for the second-order finite volume method. We propose to consider the variant introduced by Perthame–Qiu [23]. This grid is adopted since it makes easier the proof of the stability results stated in the following section. Of course, the other grid approaches, as proposed in [12], can be used. For instance, the extension to the well-known cell-center or cell-vertex grids will be seen to be obvious.

Let be given a triangulation, we denote a_i the vertexes of the triangles. The dual cell Ω_i is the volume control associated with the vertex a_i. It is delimited in joining the barycenter of all the triangles surrounding a_i (see Fig. 1). We note $\Lambda(i)$ the number of triangles surrounding a_i. For each $k \in \{1, \ldots, \Lambda(i)\}$, we set $j(k)$ the index of the cell $\Omega_{j(k)}$ neighboring Ω_i (for short, we omit the dependence on i for $j(k)$). We note $\Gamma_{ij(k)}$ the segment which separates Ω_i and $\Omega_{j(k)}$, and $\mathbf{n}_{ij(k)}$ the outer unit normal to $\Gamma_{ij(k)}$. In the sequel, $|\Omega_i|$ is the area of the cell Ω_i while $|\Gamma_{ij(k)}|$ is the length of the segment $\Gamma_{ij(k)}$. It will be useful, in the sequel, to label the mass center of the triangles. We set M_{ijk} the mass center of the triangle (a_i, a_j, a_k).

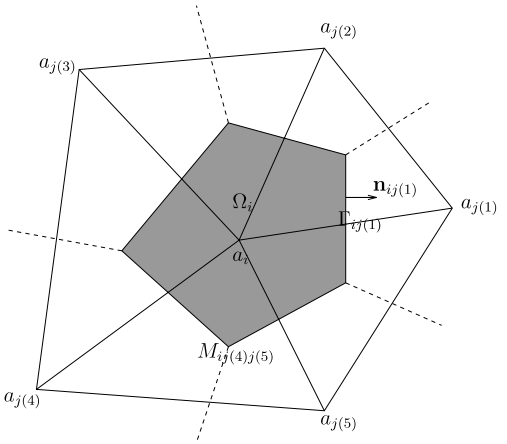

Fig. 1. Cell-center control volume: dual cell Ω_i.

Now, we give the finite volume scheme to approximate the solutions of (1). The reader is referred to [12] to complementary details. We set $\mathbf{W}_i^n$ an average of $\mathbf{W}(x, t)$ at time t^n in the dual-cell Ω_i. The sequence $\left(\mathbf{W}_i^n\right)_{i\in\mathbb{Z}}$ is evolved in time as follows:

$$|\Omega_i|\frac{\mathbf{W}_i^{n+1}-\mathbf{W}_i^n}{\Delta t}+\sum_{k=1}^{\Lambda(i)}|\Gamma_{ij(k)}|\phi\left(\mathbf{n}_{ij(k)},\mathbf{W}_{ij(k)},\mathbf{W}_{j(k)i}\right)=0, \tag{3}$$

where $\mathbf{W}_{ij}$ and $\mathbf{W}_{ji}$ are second-order approximations of the solution on each side of the edge Γ_{ij}. The limitation procedure to be applied in the construction of $\mathbf{W}_{ij}$ is detailed latter on.

As usual, the numerical flux function $\phi(\mathbf{n}, \mathbf{W}_L, \mathbf{W}_R)$ is assumed to be locally Lipschitz-continuous and satisfies

- consistency: $\phi(\mathbf{n}, \mathbf{W}, \mathbf{W}) = \mathbf{F}(\mathbf{W})\cdot\mathbf{n}$,
- conservation: $\phi(\mathbf{n}, \mathbf{W}_L, \mathbf{W}_R) = -\phi(-\mathbf{n}, \mathbf{W}_R, \mathbf{W}_L)$.

After this brief presentation of the MUSCL scheme, we turn considering the main motivation of this section. Following the ideas introduced by Berthon [3], we propose to write the scheme (3) as a relevant average of states obtained by a first-order scheme. To access such an issue, we split the dual cell Ω_i as displayed in Fig. 2. The edges $a_iM_{ij(k)j(k+1)}$ are split into two segments separated by the new vertex $m_{ij(k)j(k+1)}$. To fix the idea, we assume that $m_{ij(k)j(k+1)}$ is the middle of the segment $a_iM_{ij(k)j(k+1)}$. In fact, in the present work, the location of the vertex $m_{ij(k)j(k+1)}$ in the open segment $a_iM_{ij(k)j(k+1)}$ is free. Better choices will be given latter on.

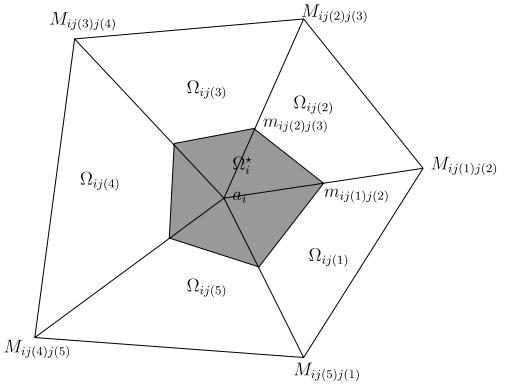

Fig. 2. Sub-cell decomposition of the dual-cell Ω_i.

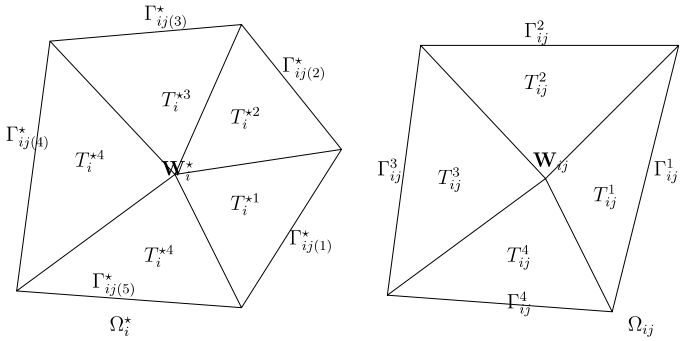

Fig. 3. Cells $\Omega_i^\star$ and Ω_{ij} as the disjoint union of triangles.

Next, we introduce $\Omega_i^\star$ a sub-cell delimited in joining $m_{ij(k)j(k+1)}$ (see Fig. 2). We note $\Omega_{ij(k)}$ the sub-cell delimited in joining the vertexes $M_{ij(k-1)j(k)}$, $M_{ij(k)j(k+1)}$, $m_{ij(k)j(k+1)}$, $m_{ij(k-1)j(k)}$. By construction, we have

$$\Omega_i = \Omega_i^\star \cup \left(\cup_{k=1}^{\Lambda(i)} \Omega_{ij(k)}\right).$$

For each sub-cell $\Omega_{ij(k)}$, we associate the second-order inner approximate state $\mathbf{W}_{ij(k)}$. We introduce the intermediate state vector $\mathbf{W}_i^\star$, associated to the sub-cell $\Omega_i^\star$, uniquely defined as follows:

$$\frac{|\Omega_i^\star|}{|\Omega_i|}\mathbf{W}_i^\star + \sum_{k=1}^{\Lambda(i)} \frac{|\Omega_{ij(k)}|}{|\Omega_i|}\mathbf{W}_{ij(k)} = \mathbf{W}_i^n. \tag{4}$$

In fact, $\mathbf{W}_i^n$ is understood as a convex combination of the vectors $\mathbf{W}_i^\star$ and $\mathbf{W}_{ij(k)}$. Now, on the split grid, we propose to evolve in time these states using the basic first-order version of the scheme (3):

$$|\Omega_i^\star|\frac{\mathbf{W}_i^{n+1,\star} - \mathbf{W}_i^\star}{\Delta t} + \sum_{k=1}^{\Lambda(i)} |\Gamma^\star_{ij(k)}| \phi\left(\mathbf{n}^\star_{ij(k)}, \mathbf{W}_i^\star, \mathbf{W}_{ij(k)}\right) = 0, \tag{5}$$

$$|\Omega_{ij(k)}|\frac{\mathbf{W}_{ij(k)}^{n+1} - \mathbf{W}_{ij(k)}}{\Delta t} + \sum_{k=1}^{4} |\Gamma^k_{ij}| \phi\left(\mathbf{n}^k_{ij}, \mathbf{W}_{ij(k)}, \mathbf{W}^k_{ij}\right) = 0, \tag{6}$$

where $\Gamma^\star_{ij(k)}$ is the segment separating $\Omega_i^\star$ and $\Omega_{ij(k)}$, and $\mathbf{n}^\star_{ij(k)}$ the outer unit normal. With some abuse in the notations, we have $\cup\Gamma^k_{ij} = \partial\Omega_{ij(k)}$ and $\mathbf{W}^k_{ij}$ denotes the values of $\mathbf{W}$ in the neighboring cells of $\Omega_{ij(k)}$ (see Fig. 3).

We immediately deduce that the updated solution $\mathbf{W}_i^{n+1}$, obtained by the classical MUSCL scheme (3) is nothing but the following average:

$$\mathbf{W}_i^{n+1} = \frac{|\Omega_i^\star|}{|\Omega_i|}\mathbf{W}_i^{n+1,\star} + \sum_{k=1}^{\Lambda(i)} \frac{|\Omega_{ij(k)}|}{|\Omega_i|}\mathbf{W}_{ij(k)}^{n+1}. \tag{7}$$

This formulation of the second-order scheme is central to establish the expected stability properties.

To conclude this brief presentation, we just assume that the sub-cells are the disjoint union of triangle T^l_{ij}, resp. $T_i^{\star l}$ as displayed in Fig. 3.

3. Stability analysis

With a large benefit, we use the decomposition (7) of the scheme (3). Indeed, considering a second-order approximation of the solution on each side of the edges Γ_{ij}, we are able to construct a relevant sub-grid in order to write the scheme (3) as a first-order average scheme on the sub-grid. Let us note from now on that, from a practical point of view, the sub-grid will never be computed. This is a crucial point since it does not increase the cost of the method. It will be seen that solely the ratio $|\Omega_i^\star|/|\Omega_i|$ and $|\Omega_{ij}|/|\Omega_i|$ are useful.

As a consequence, we have just to consider stability analysis for the first-order scheme on the sub-grid immediately to deduce similar results to the second-order scheme. In this way, we recall that the first-order 1D scheme derived from (3) reads as follows:

$$\mathbf{W}_i^{n+1} = \mathbf{W}_i^n - \frac{\Delta t}{\Delta x_i}\left(\phi\left(\mathbf{n}_x, \mathbf{W}_i^n, \mathbf{W}_{i+1}^n\right) - \phi\left(-\mathbf{n}_x, \mathbf{W}_i^n, \mathbf{W}_{i-1}^n\right)\right). \tag{8}$$

The time step Δt satisfies the first-order CFL restriction:

$$\frac{\Delta t}{\min\limits_{i\in\mathbb{Z}} \Delta x_i} \max_{i\in\mathbb{Z}} \left|\lambda\left(\mathbf{n}_x, \mathbf{W}_i^n, \mathbf{W}_{i+1}^n\right)\right| \leqslant \frac{1}{2}, \tag{9}$$

where $\lambda(\mathbf{n}, \mathbf{W}_L, \mathbf{W}_R)$ denotes, with some abuse in the notation, the numerical eigenvalues associated to the flux function $\mathbf{F}$ evaluated at $(\mathbf{n}, \mathbf{W}_L, \mathbf{W}_R)$. Since it will be useful in the sequel, let us note that the CFL number involved in (9) becomes 1 instead of 1/2 as soon as we have $\mathbf{W}_i^n = \mathbf{W}_{i+1}^n$ in (8).

In the sequel, the 1D scheme (8) is assumed to satisfy:

H1: If $\mathbf{W}_i^n \in \mathscr{V}$ then $\mathbf{W}_i^{n+1} \in \mathscr{V}$ for all i in $\mathbb{Z}$

H2: For all i in $\mathbb{Z}$, the following entropy inequalities are satisfied:

$$\frac{S\left(\mathbf{W}_i^{n+1}\right) - S\left(\mathbf{W}_i^n\right)}{\Delta t} + \frac{1}{\Delta x_i}\left(\mathscr{F}\left(\mathbf{n}_x, \mathbf{W}_i^n, \mathbf{W}_{i+1}^n\right) + \mathscr{F}\left(-\mathbf{n}_x, \mathbf{W}_i^n, \mathbf{W}_{i-1}^n\right)\right) \leqslant 0, \tag{10}$$

where $\mathscr{F}(\mathbf{n}, \mathbf{W}_L, \mathbf{W}_R)$ denotes the entropy numerical flux function.

Now, we prove that these two stability properties are preserved by the second-order 2D scheme (3) as long as a relevant CFL condition and a limitation procedure are considered.

Theorem 1. *Let us consider the second-order 2D scheme (3) and assume that all the states $\mathbf{W}_{ij}$ and $\mathbf{W}_i^\star$ belong to $\mathscr{V}$. Consider the CFL condition*

$$\Delta t \frac{\left|\Gamma_{ij}^k\right|}{\left|T_{ij}^k\right|} \max\left|\lambda\left(\mathbf{n}_{ij}^k, \mathbf{W}_{ij}, \mathbf{W}_{ij}^k\right)\right| \leqslant 1 \quad \forall \Omega_{ij},\ \ T_{ij}^k,\ 1 \leqslant k \leqslant 4, \tag{11}$$

$$\Delta t \frac{\left|\Gamma_{ij(k)}^\star\right|}{\left|T_{ij(k)}^\star\right|} \max\left|\lambda(\mathbf{n}_{ij(k)}^\star, \mathbf{W}_i^\star, \mathbf{W}_{ij(k)}\right| \leqslant 1 \quad \forall \Omega_i^\star,\ \ T_{ij(k)}^\star,\ 1 \leqslant k \leqslant \Lambda(i). \tag{12}$$

If the numerical flux function satisfies H1 for the reduced first-order scheme (8) then H1 is also satisfied by the full scheme (3).

In addition, assume H2 for the reduced scheme (8), then the second-order scheme (3) satisfies the following entropy inequalities:

$$\frac{1}{\Delta t}\left(S\left(\mathbf{W}_i^{n+1}\right) - S_i^n\right) + \frac{1}{\Omega_i}\sum_{k=1}^{\Lambda(i)} |\Gamma_{ij(k)}| \mathscr{F}\left(\mathbf{n}_{ij(k)}, \mathbf{W}_{ij(k)}, \mathbf{W}_{j(k)i}\right) \leqslant 0, \tag{13}$$

where S_i^n is defined as follows:

$$S_i^n = \frac{\Omega_i^\star}{\Omega_i} S\left(\mathbf{W}_i^\star\right) + \sum_{k=1}^{\Lambda(i)} \frac{\Omega_{ij(k)}}{\Omega_i} S\left(\mathbf{W}_{ij(k)}\right). \tag{14}$$

The first point we want highlight concerns the entropy inequalities and the definition of S_i^n. Indeed, one want use $S\left(\mathbf{W}_i^n\right)$ instead of S_i^n to define first-order entropy inequalities. As a consequence, a second-order error term is introduced:

$$\frac{1}{\Delta t}\left(S\left(\mathbf{W}_i^{n+1}\right) - S\left(\mathbf{W}_i^n\right)\right) + \frac{1}{\Omega_i}\sum_{k=1}^{\Lambda(i)} |\Gamma_{ij(k)}| \mathscr{F}\left(\mathbf{n}_{ij(k)}, \mathbf{W}_{ij(k)}, \mathbf{W}_{j(k)i}\right) \leqslant \frac{1}{\Delta t}\left(S_i^n - S\left(\mathbf{W}_i^n\right)\right),$$

where $S_i^n - S(\mathbf{W}_i^n)$ is positive by the Jensen inequality. In a sense to be prescribed, this error term comes from the variation in the reconstruction step. In the present work, second-order accuracy is assumed and the definition of S_i^n must be according with it (see [7]). In fact, the definition (14) we propose for S_i^n can be understood as a quadrature formula of the definition proposed by Bouchut–Bourdarias–Perthame [7].

Before we establish the above result, it seems important to give some comments. Let us note that the assumption $\mathbf{W}_{ij} \in \mathscr{V}$ and $\mathbf{W}_i^\star \in \mathscr{V}$ defines the limitation procedure. An example is given in the following section devoted to the numerical applications. We also emphasize the fact that no conservation limitations are imposed. The very discrepancy with more classical approaches [12,23] stays in this point.

Concerning the assumption H1 and H2, they are very natural and are satisfied by most of the schemes. To illustrate this purpose, we just recall that, arguing rotational invariance of the system (1), the numerical 2D flux function $\phi(\mathbf{n}, \mathbf{W}_L, \mathbf{W}_R)$ may be given by a 1D flux function stated in the direction of $\mathbf{n}$ (see [12] to additional details). In general, stability results are proved in the 1D case: as example see [17] for a kinetic scheme, [6] or [2] for a Suliciu relaxation scheme (the reader is also referred to [13] and references therein).

Let us emphasize that the CFL condition (11) and (12) may be seem unnatural. In fact, it is nothing but a usual CFL restriction stated, at this time, on the sub-grid made of dual cells Ω_{ij} and $\Omega_i^\star$. This CFL restriction is specified for each direction $\mathbf{n}_{ij}^k$ and $\mathbf{n}_{ij(k)}^\star$. At this level, we do not consider the initial mesh made of the cells Ω_i.

The following first-order integration lemma will be useful in the sequel

Lemma 2. *Let us consider a dual-cell Ω_i as given Fig. 1. Assume that Ω_i is a disjoint union of triangles T_i^k (similarly to the case displayed Fig. 3). The following two formulas are equivalent*:

$$\text{(i)}\ |\Omega_i|\frac{\mathbf{W}_i^{n+1}-\mathbf{W}_i^n}{\Delta t} + \sum_{k=1}^{\Lambda(i)} |\Gamma_{ij(k)}|\phi\left(\mathbf{n}_{ij(k)}, \mathbf{W}_i^n, \mathbf{W}_{j(k)}^n\right) = 0, \tag{15}$$

$$\text{(ii)}\ \mathbf{W}_i^{n+1} = \sum_{k=1}^{\Lambda(i)} \frac{|T_i^k|}{|\Omega_i|}\mathbf{W}_i^{n+1,T_i^k}, \tag{16}$$

$$\mathbf{W}_i^{n+1,T_i^k} = \mathbf{W}_i^n - \frac{\Delta t}{|T_i^k|}|\Gamma_{ij(k)}|\left(\phi(-\mathbf{n}_{ij(k)}, \mathbf{W}_i^n, \mathbf{W}_i^n) + \phi\left(\mathbf{n}_{ij(k)}, \mathbf{W}_i^n, \mathbf{W}_{j(k)}^n\right)\right). \tag{17}$$

Similarly to the reformulation (7), we note that the time evolution on a dual-cell rewrites as a relevant average. In (16) and (17), the average is made of first-order time evolution states since (17) coincides with the first-order scheme (8) in the direction of $\mathbf{n}_{ij(k)}$.

Proof of Lemma 2. An obvious Green formula application gives

$$\sum_{k=1}^{\Lambda(i)} |\Gamma_{ij(k)}|\mathbf{n}_{ij(k)} = 0.$$

Since $\phi(\mathbf{n}_{ij(k)}, \mathbf{W}_i^n \cdot \mathbf{W}_i^n) = \mathbf{F}(\mathbf{W}_i^n)\cdot\mathbf{n}_{ij(k)}$, we can rewrite (15) as follows:

$$|\Omega_i|\frac{\mathbf{W}_i^{n+1}-\mathbf{W}_i^n}{\Delta t} + \sum_{k=1}^{\Lambda(i)} |\Gamma_{ij(k)}|\left(\phi\left(\mathbf{n}_{ij(k)}, \mathbf{W}_i^n, \mathbf{W}_{j(k)}^n\right) - \phi(-\mathbf{n}_{ij(k)}, \mathbf{W}_i^n, \mathbf{W}_i^n)\right) = 0.$$

We obtain (16) and (17) since we have

$$|\Omega_i| = \sum_{k=1}^{\Lambda(i)} |T_i^k|.$$

The proof is achieved. □

Proof of Theorem 1. In the first step of the proof, the result is established on each sub-cell Ω_{ij} and $\Omega_i^\star$. For the sake of simplicity in the presentation, we just consider the sub-cells Ω_{ij} since the proof for $\Omega_i^\star$ is analogous.

In the sub-cells Ω_{ij}, we recall that the partial state $\mathbf{W}_{ij}$ is evolved in time using (6). Next, we apply Lemma 2 to write (6) as a sum of first-order schemes (8) stated in each direction $\mathbf{n}_{ij(k)}$ and given by

$$\mathbf{W}_{ij}^{n+1} = \sum_{k=1}^{4} \frac{|T_i^k|}{|\Omega_i|} \mathbf{W}_{ij}^{n+1,T_i^k}, \tag{18}$$

$$\mathbf{W}_{ij}^{n+1,T_{ij}^k} = \mathbf{W}_{ij} - \frac{\Delta t}{\left|T_{ij}^k\right|} \left|\Gamma_{ij}^k\right| \left(\phi\left(-\mathbf{n}_{ij}^k, \mathbf{W}_{ij}, \mathbf{W}_{ij}\right) + \phi\left(\mathbf{n}_{ij}^k, \mathbf{W}_{ji}, \mathbf{W}_{ij}^k\right)\right). \tag{19}$$

Assuming H1 for (8), the CFL condition (11) ensures that the evolved state $\mathbf{W}_{ij}^{n+1,T_{ij}^k}$ belongs to $\mathscr{V}$ as long as the vector states $\mathbf{W}_{ij}$ and $\mathbf{W}_i^\star$ belong to $\mathscr{V}$. In the same way, $\mathbf{W}_i^{n+1,\star}$ belongs to $\mathscr{V}$ when assuming the CFL condition (12). Since $\mathbf{W}_i^{n+1}$ is given by (7) and $\mathscr{V}$ is a convex set, we immediately deduce that $\mathbf{W}_i^{n+1}$ belongs to $\mathscr{V}$.

Concerning the entropy inequalities (13), once again we apply Lemma 2 to write (5) and (6) as a sum of first-order schemes (8). Next, the assumption H2 is applied to each first-order time evolution, $\mathbf{W}_i^{n+1,\star}$ and $\mathbf{W}_{ij}^{n+1}$, and we easily obtain

$$\frac{1}{\Delta t}\left(\sum_{k=1}^{\Lambda(i)}\left(\frac{|T_i^{\star k}|}{\Omega_i} S\left(\mathbf{W}_i^{n+1,T_i^{\star k}}\right) + \sum_{l=1}^{4} \frac{\left|T_{ij(k)}^l\right|}{\Omega_i} S\left(\mathbf{W}_{ij(k)}^{n+1,T_{ij(k)}^l}\right)\right) - S_i^n\right) + \frac{1}{\Omega_i}\sum_{k=1}^{\Lambda(i)} |\Gamma_{ij(k)}| \mathscr{F}\left(\mathbf{n}_{ij(k)}, \mathbf{W}_{ij(k)}, \mathbf{W}_{j(k)i}\right) \leqslant 0, \tag{20}$$

where S_i^n is defined by (14). Since the following equality holds:

$$\sum_{k=1}^{\Lambda(i)}\left(\frac{|T_i^{\star k}|}{\Omega_i} + \sum_{l=1}^{4} \frac{\left|T_{ij(k)}^l\right|}{\Omega_i}\right) = 1,$$

the convex property of the function $\mathbf{W} \to S(\mathbf{W})$ ensures

$$\sum_{k=1}^{\Lambda(i)}\left(\frac{|T_i^{\star k}|}{\Omega_i} S\left(\mathbf{W}_i^{n+1,T_i^{\star k}}\right) + \sum_{l=1}^{4} \frac{\left|T_{ij(k)}^l\right|}{\Omega_i} S\left(\mathbf{W}_{ij(k)}^{n+1,T_{ij(k)}^l}\right)\right) \geqslant S\left(\mathbf{W}_i^{n+1}\right).$$

The entropy inequalities (13) is thus established and the proof is achieved. □

4. Numerical applications

In this section, we apply the limitation reconstruction when approximating the solutions of the 2D Euler equations. The system of gas dynamics equations in two space dimensions reads:

$$\partial_t \mathbf{W} + \operatorname{div} \mathbf{F}(\mathbf{W}) = 0,$$

where the unknown vector is given by

$$\mathbf{W} = (\rho, \rho u, \rho v, \rho E),$$

and the flux function $\mathbf{F}(\mathbf{W}) = (\mathbf{F}_1(\mathbf{W}), \mathbf{F}_2(\mathbf{W}))$ is defined as follows:

$$\mathbf{F}_1(\mathbf{W}) = (\rho u, \rho u^2 + p, \rho uv, (\rho E + p)u),$$
$$\mathbf{F}_2(\mathbf{W}) = (\rho v, \rho uv, \rho v^2 + p, (\rho E + p)v),$$
$$p = (\gamma - 1)\left(\rho E - \rho \frac{u^2 + v^2}{2}\right), \quad \gamma \in (1, 3].$$

The set of admissible states is defined by

$$\mathscr{V} = \left\{ \mathbf{W} \in \mathbb{R}^4; \rho > 0, (u,v) \in \mathbb{R}^2, E - \frac{u^2+v^2}{2} > 0 \right\}.$$

After the work of Lax [20], because of the shock waves, it is known that entropy inequalities must be considered:

$$\partial_t \rho \mathscr{G}(\ln s) + \partial_x \rho \mathscr{G}(\ln s) u + \partial_y \rho \mathscr{G}(\ln s) v \leqslant 0, \quad s := s(\mathbf{W}) = \frac{p}{\rho^\gamma},$$

where $\mathscr{G}$ satisfies

$$\mathscr{G}'(y) < 0, \quad \mathscr{G}'(y) - \gamma \mathscr{G}''(y) < 0 \ \ \forall y \in \mathbb{R},$$

to enforce the convex property of $\mathbf{W} \to \rho \mathscr{G}(\ln s)$.

In addition, as proved by Tadmor [28], the specific entropy s satisfies the following minimum principle:

$$s(x, t+h) \geqslant \min\{ s(x', t); |x' - x| \leqslant \|u\|_\infty h \}. \tag{21}$$

The second-order MUSCL scheme (3) we propose in the present work is based on the Suliciu relaxation scheme (see [1,2,4–6,9]). In fact, with some benefit we use the rotational invariance of the flux function (for instance, see [12]). We consider the 1D numerical flux function $\phi_1(\mathbf{W}_\mathrm{L}, \mathbf{W}_\mathrm{R})$ in the x-direction to define

$$\phi\left(R \cdot \begin{pmatrix} 1 \\ 0 \end{pmatrix}, \mathbf{W}_\mathrm{L}, \mathbf{W}_\mathrm{R} \right) = \mathscr{R}^{-1} \phi_1(\mathscr{R} \cdot \mathbf{W}_\mathrm{L}, \mathscr{R} \cdot \mathbf{W}_\mathrm{R}),$$

for all unitary transform R with

$$\mathscr{R} \cdot \mathbf{W} = (\rho, \rho \mathscr{R} \cdot \begin{pmatrix} u \\ v \end{pmatrix}, \rho E).$$

Of course, it is not a genuinely multidimensional scheme but such a procedure is very frequently used. Our numerical procedure is thus tested in an usual context.

Let us note that the assumptions H1 and H2 are satisfied by the Suliciu relaxation scheme. In addition, the 1D first-order relaxation scheme satisfies a discrete entropy minimum principle [4]:

$$s(\mathbf{W}_i^{n+1}) \geqslant \min\left(s(\mathbf{W}_{i-1}^n), s(\mathbf{W}_i^n), s(\mathbf{W}_{i+1}^n) \right). \tag{22}$$

Now, we turn detailing the limitation procedure. We propose to consider the characteristic variables (ρ, u, v, p). First, we assume that the second-order approximation $\mathbf{W}_{ij}$ is performed using a standard gradient reconstruction (minmod, superbee, etc., see [11,12,29]). We set

$$\begin{aligned} \rho_{ij} &= \rho_i^n + \delta\rho_{ij}, \\ u_{ij} &= u_i^n + \delta u_{ij}, \\ v_{ij} &= v_i^n + \delta v_{ij}, \\ p_{ij} &= p_i^n + \delta p_{ij}, \end{aligned}$$

the standard second-order reconstruction. To apply the stability Theorem 1, we have to modify the gradient approximation $(\Delta\rho_{ij}, \Delta u_{ij}, \Delta v_{ij}, \Delta p_{ij})$ in order to enforce $\mathbf{W}_{ij} \in \mathscr{V}$ and $\mathbf{W}_i^\star \in \mathscr{V}$. We impose

$$\Delta\rho_{ij} > -\rho_i \quad \text{and} \quad \Delta p_{ij} > -p_i, \tag{23}$$

to obtain $\mathbf{W}_{ij} \in \mathscr{V}$. Concerning the state $\mathbf{W}_i^\star$, we have to enforce

$$\rho_i^\star > 0 \quad \text{and} \quad p_i^\star > 0, \tag{24}$$

where, after (4), we have

$$\mathbf{W}_i^\star = \frac{|\Omega_i|}{|\Omega_i^\star|} \mathbf{W}_i^n - \sum_{k=1}^{\Lambda(i)} \frac{|\Omega_{ij(k)}|}{|\Omega_i^\star|} \mathbf{W}_{ij(k)}. \tag{25}$$

In the present numerical application, we propose the following procedure:

(a) The density increments $\Delta\rho_{ij}$ are modified to ensure

$$\begin{cases} \rho_{ij} = \rho_i^n + \Delta\rho_{ij} > 0, \\ \rho_i^\star = \rho_i^n - \sum_{k=1}^{\Lambda(i)} \frac{|\Omega_{ij(k)}|}{|\Omega_i^\star|} \Delta\rho_{ij(k)} > 0. \end{cases} \tag{26}$$

(b) With $\Delta\rho_{ij}$ fixed in the step (a), the pressure increments Δp_{ij} are modified to ensure

$$\begin{cases} p_{ij} = p_i^n + \Delta p_{ij} > 0, \\ p_i^n - \sum_{k=1}^{\Lambda(i)} \frac{|\Omega_{ij(k)}|}{|\Omega_i^\star|} \Delta p_{ij(k)} > 0. \end{cases} \tag{27}$$

(c) With $\Delta\rho_{ij}$ and Δp_{ij} fixed in the steps (a) and (b), the velocity increments $(\Delta u_{ij}, \Delta v_{ij})$ are modified to ensure

$$p_i^\star = (\gamma - 1)\left((\rho E)_i^\star - \frac{((\rho u)_i^\star)^2}{2\rho_i^\star} - \frac{((\rho v)_i^\star)^2}{2\rho_i^\star} \right) > 0, \tag{28}$$

where $\mathbf{W}_i^\star$ is given by (25).

It is very easy to see that that the limitations (23) and (24) are satisfied at the end of the procedure (a)–(b)–(c). Moreover, let us remark that this procedure is well defined.

From now on, let us give several comments concerning this numerical procedure. First, since the conservation is not assumed for the gradient reconstruction, in general we do not have $\rho_i^\star = \rho_i^n$. To obtain the first limitation (26), we adopt a linear approach. We set $\Delta\rho_{ij} = \alpha\delta\rho_{ij}$ the modified density increment. In order to satisfy (26), the coefficient α must satisfy:

$$\begin{cases} \rho_{ij} = \rho_i^n + \alpha\delta\rho_{ij} > 0, \\ \rho_i^\star = \rho_i^n - \sum_{k=1}^{\Lambda(i)} \frac{|\Omega_{ij(k)}|}{|\Omega_i^\star|} \alpha\delta\rho_{ij(k)} > 0. \end{cases}$$

We adopt the same strategy to modify both pressure and velocity increments. We consider the same linear coefficient for both velocities; i.e. we set $\Delta u_{ij} = \beta\delta u_{ij}$ and $\Delta v_{ij} = \beta\delta v_{ij}$. This coefficient β is thus compute to enforce (28).

Of course, this numerical procedure is certainly not optimum. But it yields to very easy computations to modify the increments $\delta\rho_{ij}$, δu_{ij}, δv_{ij} and δp_{ij}. At this level, we have ensured the main stability results expected for the Euler equations. After Theorem 1, the positiveness of both density and pressure is proved. In addition, a set of entropy inequalities is satisfied. Once again, let us emphasize that the computation of the sub-grid is not useful. Indeed, in the above formulas, solely the ratios $|\Omega_i^\star|/|\Omega_i|$ and $|\Omega_{ij}|/|\Omega_i|$ are involved. For practical applications, a simple choice is given by

$$\frac{|\Omega_i^\star|}{|\Omega_i|} = \frac{|\Omega_{ij}|}{|\Omega_i|} = \frac{1}{\Lambda(i)+1}.$$

These results can be completed by a minimum entropy principle.

Theorem 3. *Let us consider the second-order 2D scheme (3) and assume that all the states $\mathbf{W}_{ij}$ and $\mathbf{W}_i^\star$ belong to $\mathscr{V}$. Consider the CFL restriction (11) and (12). Assume that the numerical flux function of the reduced first-order 1D scheme (8) satisfies the discrete entropy minimum principle (22) then we have*

$$s(\mathbf{W}_i^{n+1}) \geqslant \min_{1\leqslant k\leqslant \Lambda(i)} \left(s(\mathbf{W}_i^\star), s(\mathbf{W}_{ij(k)}), s(\mathbf{W}_{j(k)i}) \right). \tag{29}$$

Let us recall that the Suliciu relaxation scheme we use satisfies this result since we have (22) for the first-order reduced scheme.

To prove Theorem 3, we need the following technical result:

Lemma 4. *Consider the following convex sum*

$$\mathbf{W} = \sum_{k=1}^{N} \alpha_k \mathbf{W}_k, \quad \sum_{k=1}^{N} \alpha_k = 1, \quad \alpha_k \geqslant 0, \tag{30}$$

and assume the following entropy minimum principle

$$s(\mathbf{W}_k) \geqslant \min_{j \in \Theta(k)} (s(\mathbf{W}_j)),$$

where $\Theta(k)$ denotes a bounded set of admissible indexes. Then we have

$$s(\mathbf{W}) \geqslant \min_{j \in \cup_{k=1}^{N} \Theta(k)} (s(\mathbf{W}_j)). \tag{31}$$

Proof. This result is a direct consequence of the convex property of the function $\mathbf{W} \to \rho\mathscr{G}(\ln s(\mathbf{W}))$. Indeed, as long as $\mathbf{W}$ satisfies (30), we have

$$\rho\mathscr{G}(\ln s(\mathbf{W})) \leqslant \sum_{k=1}^{N} \alpha_k \rho_k \mathscr{G}(\ln s(\mathbf{W}_k)).$$

Since $\mathscr{G}$ is a decreasing function, we have

$$\begin{aligned} \mathscr{G}(\ln s(\mathbf{W}_k)) &\leqslant \mathscr{G}\left(\ln\left(in_{j \in \Theta(k)}(s(\mathbf{W}_j))\right)\right), \\ &\leqslant \mathscr{G}\left(\ln\left(\min_{j \in \cup_{k=1}^{N} \Theta(k)} (s(\mathbf{W}_j))\right)\right), \end{aligned}$$

and thus we have

$$\begin{aligned} \rho\mathscr{G}(\ln s(\mathbf{W})) &\leqslant \left(\sum_{k=1}^{N} \alpha_k \rho_k\right) \mathscr{G}\left(\ln\left(\min_{j \in \cup_{k=1}^{N} \Theta(k)} (s(\mathbf{W}_j))\right)\right), \\ &\leqslant \rho\mathscr{G}\left(\ln\left(\min_{j \in \cup_{k=1}^{N} \Theta(k)} (s(\mathbf{W}_j))\right)\right). \end{aligned}$$

The expected inequality (31) is then immediately deduced arguing, once again, the decreasing property of $\mathscr{G}$. The proof is achieved. □

Proof of Theorem 3. The proof exactly follows the establishment of Theorem 1. Once again, we apply Lemma 2 to write (5) and (6) as a sum of first-order scheme (8) for each direction $\mathbf{n}_{ij(k)}$. Under the CFL condition (11) and (12), we apply the discrete minimum principle (22) to each first-order time evolution (17). The expected discrete entropy minimum principle (29) is thus a direct consequence of Lemma 4. □

The scheme is now applied to performed several numerical tests. We recall that the Suliciu relaxation numerical flux function (see [4,5]) is used in the present paper. We have adopted this flux because it satisfies all the stability assumptions H1, H2 but also (22). The reader is referred to [22] or [17] to another scheme satisfying stability properties. Let us note that several 1D numerical flux functions satisfy H1 and H2 (for instance, see [5]). Arguing the rotational invariance, they can be applied to develop robust 2D MUSCL schemes.

All the tests are performed using the same strategy. The CFL number is fixed to 0.5 according to (11) and (12). The gradient reconstruction is performed with the so-called Superbee limiter (see [25] but also [29] and references therein). We have adopted this limiter because of its well-known accuracy and its instabilities (large oscillations) when solving the Euler equations. The Superbee approach involves large oscillations when considering standard MUSCL schemes. This makes very difficult severe numerical tests. Since our procedure makes robust the scheme, no problem will appear for severe tests. For the sake of consistency with the detailed

scheme (3), we do not involve a second-order time accuracy. Actually, many second-order accurate time procedures exist in the literature (for instance, see [3,17]) which preserve the robustness of the first-order accurate time schemes.

The two first tests are devoted to 1D problems computed on a 2D unstructured grid (see Fig. 4). The grid is made of a random triangulation where we have imposed amounts 125 nodes in the horizontal direction and amounts 25 nodes in the vertical direction. First, a classical shock tube is considered. The results are displayed in Fig. 5. Both first- and second-order numerical approximations are compared to the exact solution.

The second 1D problem concerns a very difficult problem since the density and pressure vanish. As expected, the present variant of the MUSCL scheme does not generate negative density or pressure. The numerical results are given Fig. 6 and compared to the exact solution.

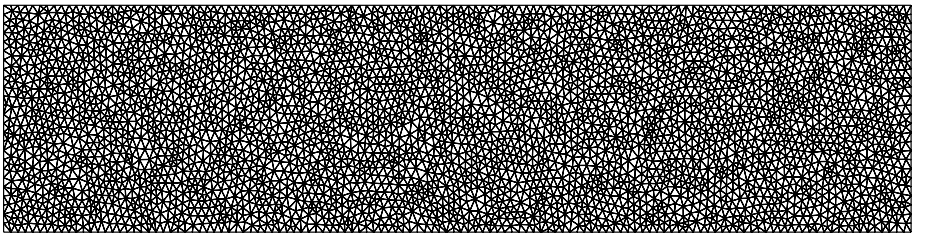

Fig. 4. A 2D unstructured mesh for the 1D problems, 3996 nodes and 7690 triangles.

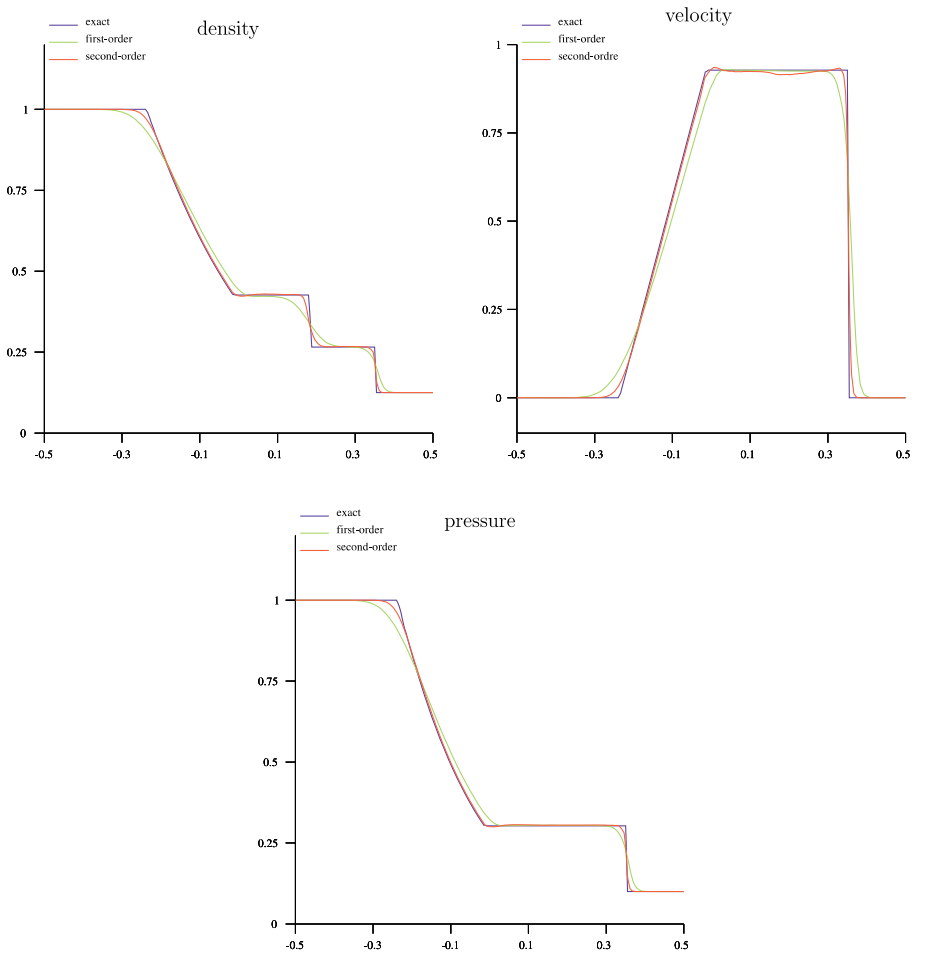

Fig. 5. Shock tube. Comparison of the exact solution and both first-order and second-order approximate solutions.

In the next numerical experiment, we consider the double Mach reflection on a ramp proposed by Woodward–Colella [30]. This test is known to be severe for the robustness and the accuracy of the schemes. It involves discontinuous flows with very complex structures. It consists of the interaction of a planar Mach 10 shock with a 30° ramp. Ahead the shock wave, the gas has density 1.4, pressure 1 with γ fixed to 1.4. The reader is referred to [30] for a detailed description of the experiment. The test is performed when considering an unstructured grid made of 47,852 nodes and 94,847 triangles which corresponds to edge's length amounts 1/100. We have considered a similar thickness as proposed in [30]. The density result is displayed Fig. 7. The obtained result is in good agreement with the results displayed in [30] (see also [24]).

We follow performing numerical experiments proposed by Woodward–Colella [30]. We consider the Mach 3 wind tunnel with a step. Initially, the wind tunnel contains a uniform gas with density 1.4, pressure 1, velocity 3 and γ fixed to 1.4. The solution of this problem involves shock waves interacting with the tunnel. The test is performed with an unstructured grid made of 20,117 nodes and 39,592 triangles which corresponds to edge's length amounts 1/80. The thickness of the grid is the same as imposed in [30]. The density and pressure results are displayed in Fig. 8.

The last numerical experiment we propose is devoted to a flow around an ellipse with a Mach number of 25, an incidence of 30° and γ fixed to 1.2. This test has been introduced in [23] and turns out to be particularly difficult since, in general, negative pressures are reported behind the body. According to the theory, the modified MUSCL scheme gives a positive solution. However, let us note that the limitation we have introduced makes the scheme robust but does not provide the oscillations. In this test, we observe a bad residue decay.

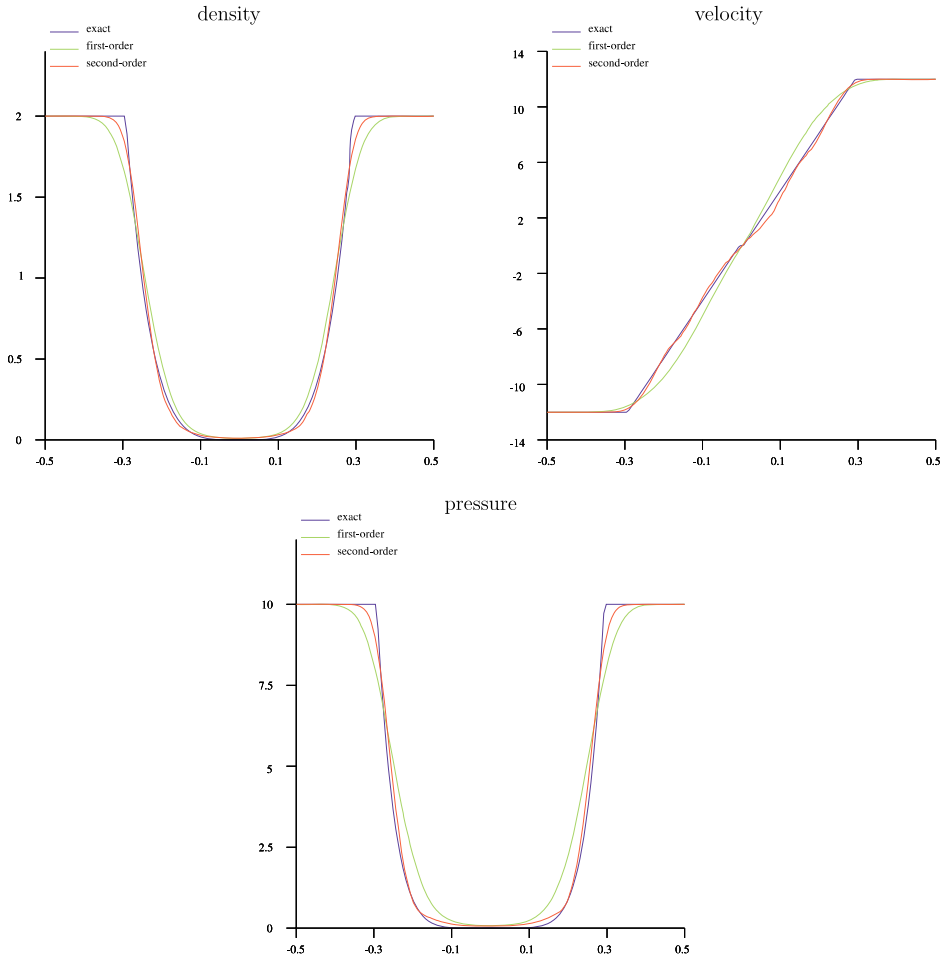

Fig. 6. Double rarefaction waves. Comparison of the exact solution and both first-order and second-order approximate solutions.

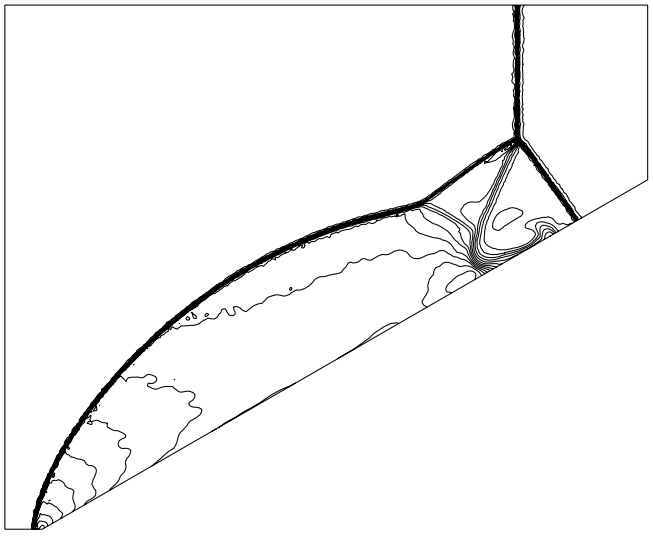

Fig. 7. Double Mach reflection. Density at time $t = 0.2$, 30 isovalues from 7.55 to 21.5.

density

To decrease this residue decay, we try several limitation approaches as prescribed in [12, pp. 412–415]. In this numerical experiment, these limitations must be separated in two families. If we do not enforce our robust procedure, most of the standard limitations involve negative pressure. The limitation procedures performing the test give near first-order results. Now, if we enforce the robustness, numerical results are obtained with both families of limitations. The results remain "first-order" when the original limitation gave "first-order" results. The remaining limitation procedures give second-order numerical approximation but for a poor residue decay. Concerning this numerical experiment, the best results are actually obtained in [23].

An adapted unstructured mesh made of 4810 nodes and 9421 triangles has been considered to perform the numerical experiment. The Mach number solution is displayed in Fig. 9 when the initial data is made of the converged first-order solution. Let us note that the same result is obtained with an initial data made of a constant state.

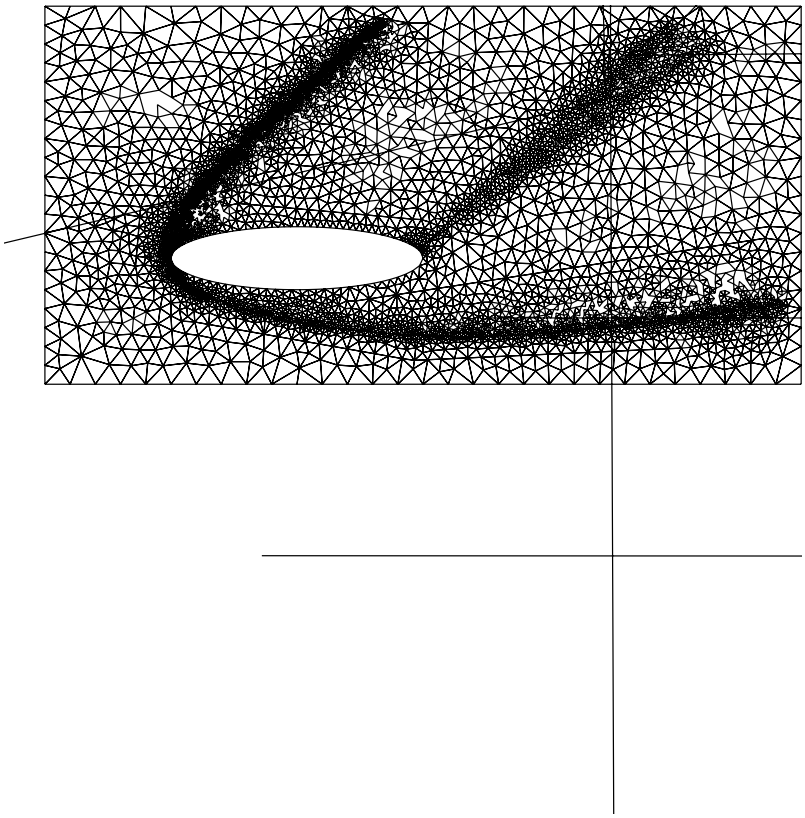

5. Conclusion

In this paper, we propose a version of the celebrate MUSCL scheme on 2D unstructured grid. These schemes are second-order accuracy but are known to be poorly robust. Arguing a relevant gradient reconstruction limitation and a relevant CFL restriction, we ensure the expected robustness. When applying to the compressible Euler equations, the resulting MUSCL scheme preserves the positiveness of both density and pressure. This robustness of the method is supplemented by a set of discrete second-order entropy inequalities. Moreover, in the context of the Euler equations, we establish a discrete entropy minimum principle. This limitation turns out to be very easy and its numerical implementation does not involve technical difficulties. In addition, this limitation can be considered with any MUSCL schemes and thus enforces the expected robustness but it does not increase the cost of the scheme. To illustrate the method, we have performed several numerical tests. In the literature, most of them are considered as severe.

References

[1] M. Baudin, C. Berthon, F. Coquel, R. Masson, H. Tran, A relaxation method for two-phase flow models with hydrodynamic closure law, Numer. Math. 99 (3) (2005) 411–440.

[2] C. Berthon, Inégalités d'entropie pour un schéma de relaxation, C.R. Acad. Sci. I, Math. 340 (2005) 63–68.

[3] C. Berthon, Stability of the MUSCL schemes for the Euler equations, Commun. Math. Sci. 3 (2005) 133–158.

[4] C. Berthon, Numerical approximations of the 10-moment Gaussian closure, Math. Comput. (accepted).

[5] F. Bouchut, Nonlinear stability of finite volume methods for hyperbolic conservation laws, and well-balanced schemes for sourcesFrontiers in Mathematics series, Birkhäuser, 2004.

[6] F. Bouchut, Entropy satisfying flux vector splittings and kinetic BGK models, Numer. Math. 94 (2003) 623–672.

[7] F. Bouchut, Ch. Bourdarias, B. Perthame, A MUSCL method satisfying all the numerical entropy inequalities, Math. Comput. 65 (216) (1996) 1439–1461.

[8] P. Colella, Multidimensional upwind methods for hyperbolic conservation laws, J. Comput. Phys. 87 (1990) 171–200.
[9] F. Coquel, B. Perthame, Relaxation of energy and approximate Riemann solvers for general pressure laws in fluid dynamics, SIAM J. Numer. Anal. 35 (6) (1998) 2223–2249.
[10] L.J. Durlofsky, B. Engquist, S. Osher, Triangle based adaptive stencils for the solution of hyperbolic conservation laws, J. Comput. Phys. 98 (1992) 64–73.
[11] E. Godlewski, P.A. Raviart, Hyperbolic systems of conservations laws, Tome 1, SMAI (Eds.), Ellipse, 1991.
[12] E. Godlewski, P.A. Raviart, Hyperbolic systems of conservations laws, Tome 2, Applied Mathematical Sciences, vol. 118, Springer, Berlin, 1995.
[13] A. Harten, P.D. Lax, B. Van Leer, On upstream differencing and Godunov-type schemes for hyperbolic conservation laws, SIAM Rev. 25 (1) (1983) 35–61.
[14] A. Harten, High resolution schemes for hyperbolic conservation laws, J. Comput. Phys. 49 (1983) 357–393.
[15] S. Jin, Z. Xin, The relaxation scheme for systems of conservation laws in arbitrary space dimension, Commun. Pure Appl. Math. 45 (1995) 235–276.
[16] S. Karni, A multicomponent flow calculations by a consistent primitive algorithm, J. Comput. Phys. 112 (1994) 31–43.
[17] B. Khobalatte, B. Perthame, Maximum principle on the entropy and second-order kinetic schemes, Math. Comput. 62 (205) (1994) 119–131.
[18] B. Larrouturou, How to preserve the mass fractions positivity when computing compressible multi-component flows, J. Comput. Phys. 95 (1991) 59–84.
[19] P.D. Lax, Hyperbolic systems of conservation laws and the mathematical theory of shock waves, Conference Board of the Mathematical Sciences Regional Conference Series in Applied Mathematics, vol. 11, SIAM, Philadelphia, 1973.
[20] P.D. Lax, Shock waves and entropy, in: Contributions to Nonlinear Functional Analysis, Academic Press, New York, 1971, pp. 603–634.
[21] B. van Leer, Towards the ultimate conservative difference scheme. V. A second-order sequel to Godunov's method, J. Comput. Phys. 32 (1979) 101–136.
[22] B. Perthame, Boltzmann type schemes for gas dynamics and the entropy property, SIAM J. Numer. Anal. 27 (6) (1990) 1405–1421.
[23] B. Perthame, Y. Qiu, A variant of Van Leer's method for multidimensional systems of conservation laws, J. Comput. Phys. 112 (2) (1994) 370–381.
[24] M. Ricchiuto, A. Csí k, H. Deconninck, Residual distribution for general time-dependent conservation laws, J. Comput. Phys. 1 (2005) 249–289.
[25] P.L. Roe, Generalized formulation of TVD Lax–Wendroff schemes, Technical Report ICASE 84-53, NASA Langley Research Center, Hampton, USA, 1984.
[26] P. Rostand, B. Stoufflet, TVD schemes to compute compressible viscous flows on unstructured meshes, Nonlinear hyperbolic equations-theory, computation methods, and applications, in: Proceedings of the Second International Conference on Aachen/FRG 1988, Notes Numer. Fluid Mech., vol. 24, 1989, pp. 510–520.
[27] R. Sanders, A. Weiser, High resolution staggered mesh approach for nonlinear hyperbolic systems of conservation laws, J. Comput. Phys. 101 (1992) 314–329.
[28] E. Tadmor, A minimum entropy principle in the gas dynamics equations, Appl. Numer. Math. 2 (3–5) (1986) 211–219.
[29] E.F. Toro, Riemann solvers and numerical methods for fluid dynamics, second ed.A Practical Introduction, Springer, Berlin, 1999.
[30] P. Woodward, P. Colella, The numerical simulation of two-dimensional fluid flow with strong shocks, J. Comput. Phys. 54 (1984) 115–173.